Drape Modelling of Multi-Layered Composites

E.A.D. Lamers, S.Wijskamp, R. Akkerman

University of Twente, Department of Mechanical Engineering, Composites Group, PO Box 217, 7500 AE Enschede, the Netherlands

URL: www.composites.ctw.utwente.nl
e-mail: E.A.D.Lamers@ctw.utwente.nl, S.Wijskamp@ctw.utwente.nl, R.Akkerman@ctw.utwente.nl

ABSTRACT: In order to predict product distortions when producing thermoplastic composite parts in the Rubber Press Forming process, the occurring fibre re-orientation must be known. From drape experiments on a double dome geometry it is clear that the interlaminar shear behaviour has a dominating effect on the drape behaviour of multi-layered composites. A multi-layer material model, incorporating this interlaminar shear, was implemented into the FE-package DiekA. The predicted fibre distribution was then compared with the experimental results.

Key words: composites, draping, FE-draping, composites forming

1 INTRODUCTION

The Rubber Press Forming process (RPF) is a relatively fast process for fabric-reinforced thermoplastics. Typically, the production cycle is in the order of a few minutes and consists of infrared heating of a multi-layer preform above melt or glass transition temperature, hot pressing of the preform and cooling the preform below the glass transition temperature of the thermoplastic matrix. The negatively shaped rubber upper mould presses the hot preform on a positively shaped steel lower mould. During pressing the rubber deforms nearly hydrostatically, proving a good way to consolidate the laminate. Heating, pressing, cooling and removing the product from the press are automated, ensuring reproducibility.
However, production may lead to shrinkage and warpage, resulting in unacceptable dimensional changes of the products. Fibre re-orientation is one of the major factors causing these distortions. Especially when producing doubly curved parts, the process of draping causes the angle between the warp and weft yarns to vary over the product with this double curvature. Obviously, the resulting fibre orientations must be predicted accurately to predict the overall properties of the product, since the properties and the orientation of the fibres dominate the composite's material behaviour.
Several authors [1, 2, 3] modelled the draping process using FE methods. One of the main reasons for this was the incapability of the geometrical method to incorporate the inter-ply composite properties and processing conditions during draping. The inter-ply composite behaviour can have a dominating effect on the drape properties, as shown by Lamers *et al.* [3].
Here, a multi-layer fabric-reinforced fluid was implemented in DIEKA, a Finite Element (FE) package used for modelling forming processes, such as e.g. deep drawing of metals. Using different lay-ups, drape experiments were performed on a double dome geometry. Finally, the results of the FE-model are compared with experimental results.

2 FE DRAPING

De Luca *et al.* [1] developed a multi-layer drape approach using "specialised viscous-friction and contact constraints" between the shell elements of the drape material, to incorporate the inter-ply composite shear phenomenon in FE simulations. This method leads to computationally expensive FE simulations, since the number of Degrees of Freedom (DOF) increases dramatically with the number of layers in the composite. Here, a material model is presented incorporating the inter-ply composite behaviour. With this model, only one sheet element is required through the thickness of the laminate for modelling the drape of multi-layered composites.

2.1 Single layer drape material model

For single-layer composites, Lamers *et al.* [3] implemented a material model similar to the model developed by Spencer [4]. Finite fibre stiffness in the fibre direction, and compressible matrix behaviour are assumed in the model. The fibres are assumed to have only stiffness properties in the fibre directions and the matrix response is Newtonian viscous. The total Cauchy stress $\boldsymbol{\sigma}$ is hence expressed as:

$$\boldsymbol{\sigma} = \boldsymbol{\sigma}_e + \boldsymbol{\tau}(\boldsymbol{D},\boldsymbol{a},\boldsymbol{b}), \tag{1}$$

with

$$\boldsymbol{\sigma}_e = -p\boldsymbol{I} + S_a V_{f1}\boldsymbol{A} + S_b V_{f2}\boldsymbol{B},$$

and

$$\begin{aligned}\boldsymbol{\tau}(\boldsymbol{D},\boldsymbol{a},\boldsymbol{b}) = V_m\big(&2\eta\boldsymbol{D} + 2\eta_1(\boldsymbol{A}\cdot\boldsymbol{D} + \boldsymbol{D}\cdot\boldsymbol{A}) + \\ &2\eta_2(\boldsymbol{B}\cdot\boldsymbol{D} + \boldsymbol{D}\cdot\boldsymbol{B}) + 2\eta_3(\boldsymbol{E}\cdot\boldsymbol{D} + \boldsymbol{D}\cdot\boldsymbol{E}^T) + \\ &2\eta_4(\boldsymbol{E}^T\cdot\boldsymbol{D} + \boldsymbol{D}\cdot\boldsymbol{E})\big)\end{aligned}$$

where

$$\boldsymbol{A} = \boldsymbol{aa}, \quad \boldsymbol{B} = \boldsymbol{bb}, \quad \boldsymbol{E} = \boldsymbol{ab}$$

In these equations, $\boldsymbol{\sigma}_e$ and $\boldsymbol{\tau}$ are stresses, $\boldsymbol{D}$ is the rate of deformation tensor, p is the hydrostatic pressure, $S_{a,b}$ are the fibre longitudinal stresses, and the vectors $\boldsymbol{a}$ and $\boldsymbol{b}$ represent the fibre directions. η, η_1, η_2, η_3 and η_4 are composite viscosities that depend on the angle between the fibre directions. V_{f1}, V_{f2} and V_m are the volume fractions of respectively the two fibre directions and the matrix.

2.2 Multi-layer drape material model

To incorporate inter-ply behaviour of multi-layered composites, the individual plies in the material must slide with respect to each other and deform individually. Figure 1 illustrates the deformation of a three ply laminate of biaxial fabrics. In the original configuration, the plies have two independent fibre orientations $\boldsymbol{a}^i$ and $\boldsymbol{b}^i$ (where i is the ply index).

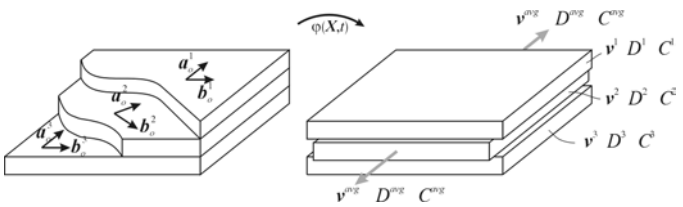

Fig 1: Individual and averaged ply deformations of a three layer laminate

For a given average deformation, the plies are allowed to deform individually, conforming to their fibre orientations. As a result, also the velocity and the rate of deformation will, generally, be non-uniform over the laminate thickness. The Cauchy-Green deformation and rate of deformation, $\boldsymbol{C}^i$ and $\boldsymbol{D}^i$ respectively, are assumed to be piecewise constant for each ply i in an element.
The element through-thickness average deformation, rate of deformation and velocity are denoted as, $\boldsymbol{C}^{avg}$, $\boldsymbol{D}^{avg}$ and $\boldsymbol{v}^{avg}$ respectively. These averaged values correspond to the nodal displacement increments in the finite element representation. The individual ply deformations are then found by minimising the total power in the element.

2.2.a Ply contribution

For each ply an inplane displacement field is assumed under the assumption of plane stress as:

$$\begin{aligned}\Delta u_x^i &= a_1^i + a_2^i\Delta x + a_3^i\Delta y \\ \Delta u_y^i &= b_1^i + b_2^i\Delta x + b_3^i\Delta y\end{aligned}, \tag{2}$$

where Δu_x^i and Δu_y^i are the displacement increments in x- and y-direction, a_1^i, a_2^i, a_3^i, b_1^i, b_2^i and b_3^i are constants in each ply i. Discretising in time leads to:

$$\begin{aligned}v_x^i &= (a_1^i + a_2^i\Delta x + a_3^i\Delta y)/\Delta t \\ v_y^i &= (b_1^i + b_2^i\Delta x + b_3^i\Delta y)/\Delta t\end{aligned}, \tag{3}$$

resulting in the velocity components v_x^i and v_y^i.
From equation (3), the rates of deformation can be derived in terms of, a_1^i, a_2^i, a_3^i, b_1^i, b_2^i and b_3^i.
Using the material model (1), the power contribution P_{ly}^i per ply can be derived as:

$$P_{ply}^i = \int_{\Omega^i} \boldsymbol{\sigma}^i : \boldsymbol{D}^i \, d\Omega^i, \tag{4}$$

where Ω^i is the volume of the ply i in the element.

2.2.b Velocity difference between layers

Since the individual plies in the laminate can have different velocities, the interface between these plies must deform correspondingly. Assuming resin rich layers between the individual plies in the laminate, the interlaminar behaviour is assumed to be viscous, leading to a viscous slip law expressed in the velocity differences between subsequent layers. This can be elaborated to the power P_{int}^j as:

$$P_{int}^j = \int_{\Phi^j} \boldsymbol{\xi}^j \cdot \boldsymbol{v}_{rel}^j \, d\Phi^j, \tag{5}$$

where Φ^j is the area of the slip surface and $\boldsymbol{\xi}^j$ is the

corresponding constant slip vector.

2.2.c Stresses acting on plies

The edges of the individual plies will be subjected to an external stress from the adjacent elements. In the FE simulation, these stresses are assumed to act in the fibre directions $\boldsymbol{a}^i$ and $\boldsymbol{b}^i$, resulting in a power contribution $P_{tr}{}^k$ per ply as:

$$P_{tr}^k = \int_{\Gamma^k} \boldsymbol{t}^k \cdot \boldsymbol{v}^k \, d\Gamma^k \,, \tag{6}$$

where $\boldsymbol{t}^k$ is the traction induced by the stresses acting on the sides k of the ply with area Γ^k. In the FE implementation only the components in the fibre direction are evaluated, as the other components can be assumed to be negligible.

2.2.d Ply deformations

Combining (4), (5) and (6), the power P adds up to:

$$P = \sum_{i=1}^{n} P_{ply}^i + \sum_{j=1}^{n-1} P_{int}^j + \sum_{i=1}^{n} \sum_{k=1}^{s} P_{tr}^{k^i} \,, \tag{7}$$

where n stands for the number of plies and s for the number of sides of the element. Minimizing P for $a_1{}^i$, $a_2{}^i$, $a_3{}^i$, $b_1{}^i$, $b_2{}^i$ and $b_3{}^i$ results in:

$$\frac{\partial P}{\partial q} = 0 \,, \qquad \text{(where } q = a_l{}^i, b_l{}^i \text{ with } l = 1,2,3\text{)} \tag{8}$$

Using 8 and the constraints:

$$\boldsymbol{v}^{avg} = \sum_{i=1}^{n} \tfrac{1}{n} \boldsymbol{v}^i \,, \quad \boldsymbol{D}^{avg} = \sum_{i=1}^{n} \tfrac{1}{n} \boldsymbol{D}^i \quad \text{and} \quad \boldsymbol{C}^{avg} = \sum_{i=1}^{n} \tfrac{1}{n} \boldsymbol{C}^i \,, \tag{9}$$

a linear system with the unknowns $a_1{}^i$, $a_2{}^i$, $a_3{}^i$, $b_1{}^i$, $b_2{}^i$ and $b_3{}^i$ is formed. This system can be solved straightforwardly, eventually resulting in the individual ply deformations.

2.3 FE Implementation

Linear triangular membrane elements with one integration point were used to implement the material model in DIEKA.

Contact was modelled using a regularisation method Kloosterman [5]. A penalty approach was used to model the normal contact between the composite and the moulds. Viscous sliding friction between the moulds and the composite was used with a constant slip coefficient.

The drape simulation is displacement controlled by moving the steel mould towards the rubber mould in small steps. For each displacement step, the system is solved using a predictor-corrector scheme (implicit). The simulations stops when the rubber mould reaches the steel mould.

Due to the individual ply deformations, the fibres in these plies also change direction. In order to find the orientations in the average configuration, a remap of the fibre directions is required, as illustrated in figure 2.

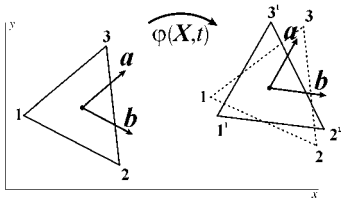

Fig 2: Remap of the fibre orientations from deformed ply onto the average deformation

The element is deformed from the initial configuration to the dotted current configuration. The fibre directions $\boldsymbol{a}$ and $\boldsymbol{b}$ are mapped from the individual ply topography (nodes 1^i, 2^i and 3^i) in the current configuration, onto the average element topography (nodes 1, 2 and 3).

From figures 1 and 2, it is obvious that individual layers move across the element boundaries into the neighbouring elements. To account for these convective terms, an ALE scheme as described by Van Haaren [6], will be implemented in the model.

3 EXPERIMENTS

Rubber press experiments on a double dome geometry were performed at Stork/Fokker Special Products using Ten Cate Advanced Composites Cetex® materials, see Lamers *et al.* [3]. The product shape consists of two intersecting hemispheres with different radii.

Three configurations of Satin 8H glass fibre reinforced poly(phenylenesulfide) (PPS) laminates were pressed, a $[0°/90°]_{2s}$, $[45°/-45°]_{2s}$ and a Quasi-Isotropic (QI) $[0°/90°/45°/-45°]_s$ lay-up.

The experimental results are shown in figure 3. It is obvious from the experiments that the main fabric (shear) deformation occurs for both the $[0^o/90^o]_{2s}$ and the $[45^o/-45^o]_{2s}$ lay-up in the directions marked with an **S** in figure 3. However, the QI lay-up behaves completely differently. This laminate wrinkles (black arrows in figure 3) and shows far less shear deformation than the other two laminates, as the different deform abilities of the separate layers is restricted by the interlaminar transverse shear stiffness of the laminate.

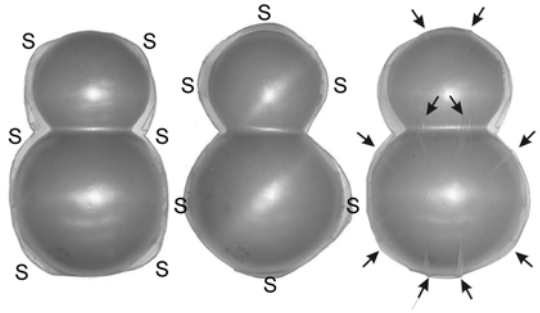

Fig 3: RPF laminates, $[0°/90°]_{2s}$, $[45°/-45°]_{2s}$ and a QI lay-up

4 SIMULATIONS

Draping was simulated using an unstructured mesh of 4098 membrane elements. The longitudinal modulus of the glass fibres (65 GPa) was used as an input parameter for the Satin 8H glass fabric. The estimated input parameters for the PPS polymer matrix were: η=100, $\eta_1=\eta_2$=30, $\eta_3=\eta_4$=10 Pa·s. The inter-ply slip coefficient was set at 33 m/(Pa·s) and the fibre volume fraction at 50%. The initial fibre directions were the same as in the experiments and the slip coefficient was set at 33 m/(Pa·s) for both the composite/tools contacts. The results are depicted in figure 4.

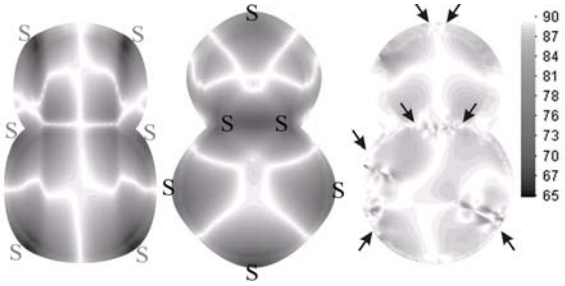

Fig 4: Simulation results, $[0°/90°]_{2s}$, $[45°/-45°]_{2s}$ and QI lay-up

5 DISCUSSION

The single-layer drape material model was well able to predict the fibre re-orientations of the $[0^o/90^o]_{2s}$ and $[45^o/-45^o]_{2s}$ products, as shown in [3]. For the QI lay-up the multi-layer FE drape simulation predicts the wrinkles in the areas observed in the experiments. However, the simulation predicts a asymmetric wrinkling pattern, which is not found in the experiments. Assuming even functions for the composite viscosities, resulting in an asymmetric fabric shear response (see Spencer [4]) probably causes this.

The simulation time for the single-layer material model is 40 minutes while the multi-layer model used 65 minutes on an Athlon XP2000+ PC.

Using two layers of shell elements in a simulation would already have doubled the DOF's in the simulation, increasing the CPU time with a factor of 2.5 at least. The multi-layer drape material model described here clearly has a speed benefit compared to such a model.

Convection of the individual plies across element boundaries will be taken into account in this simulation. To improve the accuracy of the model, an upwind convection scheme is currently being implemented.

Currently pictureframe test are being performed in order to gather the required input data for the model. Additionally, fabric pullout tests are done to determine the inter-ply composite behaviour.

6 CONCLUSIONS

A multi-layer drape material model was developed and implemented in the FE package DIEKA. It incorporates a biaxial fabric in a Newtonian viscous like matrix material, using a constant slip law between the individual layers. Drape simulations of the Rubber Press Forming process were performed successfully. The material model provides a computationally attractive tool to model draping of multi-layered composites. The results were compared with experiments and confirm the clear dependency between the drape behaviour and the laminate lay-up.

REFERENCES

1. P. de Luca, P. Lefébure and A.K. Pickett, Numerical and experimental investigation of some press forming parameters of two fibre reinforced thermoplastics: APC2-AS4 and PEI-cetex, *Composites: Part A*, vol. 29A (1998) 101-110.
2. S.P. McEntee and C.M. Ó Brádaigh, Large deformation finite element modelling of single-curvature composite sheet forming with tool contact, Composites: Part A, vol. 29A (1998) 207-213.
3. E.A.D. Lamers, S. Wijskamp & R. Akkerman, Fibre Orientation Modelling for Rubber Press Forming of Thermoplastic Laminates, *Esaform 2002,* 323-326.
4. A.J.M. Spencer, Theory of fabric-reinforced viscous fluids, *Composites: Part A*, vol. 31 (2000) 1311-132.
5. G. Kloosterman, *Contact methods in Finite Element Simulations (Ph.D Thesis*), University of Twente, the Netherlands, Dec. 2002.
6. M.J. van Haaren, H.C. Stoker, A.H. van den Boogaard and H. Huéting, The ALE-method with triangular elements: direct convection of the integration point values, *Int. J. Numer. Meth. Engng. 2000*, 49, 697-720.